Eur. J. Mech., B/Fluids, **8**, n° 5, 375-396, 1989

Hydrodynamical regimes in metallic melts subject to a horizontal temperature gradient

B. ROUX *, H. BEN HADID * and P. LAURE **

ABSTRACT. — The flow structure of a low-Prandtl-number fluid in open horizontal cavities has been emphasized by numerical simulation and stability analysis. We mainly considered natural convection alone, for which 2D-oscillatory regimes have been found for infinitely long cavities (by a stability analysis) and for cavities with moderate aspect ratios, A (by numerical simulations performed for $A=4$). Such 2D-oscillatory regimes also exist for $Pr=0$; they are essentially of dynamical origin. We also considered the numerical simulation of the thermocapillary-driven convection in a rectangular cavity with $A=4$. The computed 2D-flow is steady up to $Ma=500$ (at least), and exhibits a "flywheel" structure for high Ma. For small Ma, the Couette flow solution can be established in the core of the cavity. A few results concerning the coupling between the two previous modes of convection, have been given in the case where the buoyancy effect is dominant. For positive Ma, the stability threshold for 2D-oscillatory regimes induced by buoyancy, Gr_c, increases with Ma. For small negative Ma, Gr_c dimishes when $|Ma|$ increases, but a re-stabilization has to be expected for large $|Ma|$.

1. Introduction

This study concerns the behaviour of fluid layers in open parallelepipedic cavities of large horizontal extent, subject to a horizontal temperature gradient (see *Fig.* 1). The fluid motion is generated by volume forces (natural convection) and/or surface forces

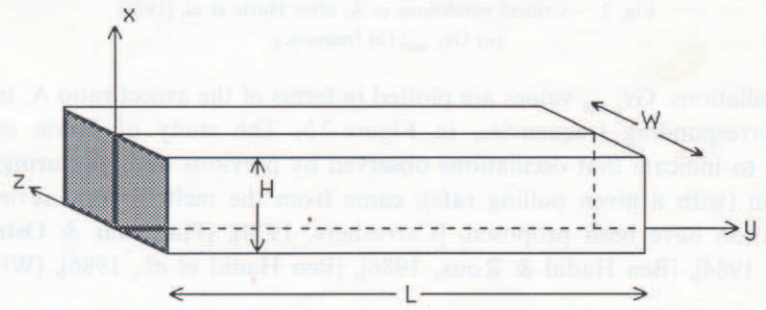

Fig. 1. — Geometry of the problem.

* Institut de Mécanique des Fluides, UM-34 du C.N.R.S., 1, rue Honnorat, 13003 Marseille, France.
** Département de Mathématiques, Université de Nice, Parc Valrose, 06034 Nice Cedex, France.

EUROPEAN JOURNAL OF MECHANICS, B/FLUIDS, VOL. 8, N° 5, 1989
0997-7546/89/05 375 22/$ 4.20/

(thermocapillary convection), due to this temperature gradient. The respective influence of these two types of convection has been studied on the basis of an order of magnitude analysis by Napolitano [1982], for a large variety of cases.

We are interested here in the onset of oscillatory regimes in metallic melts which correspond to low-Prandtl-number fluids, Pr. This study has been motivated by experiments carried out by Favier and his co-workers [1987], on directional solidification by the horizontal Bridgman technique, and on the thermocapillary convection [Camel *et al.*, 1986]. It is well known that thermal oscillations are detrimental to monocrystals, as they generate striations [Hurle, 1967]. Numerous studies have already been devoted to this subject, more than twenty years ago, mainly by Cole & Winegard [1964], Hurle [1967], Utech *et al.*, [1967], Carruthers & Winegard [1967] and Carruthers [1968], in the cases of open or closed cavities.

Fundamental studies, from the hydrodynamic point of view, have been carried out, without pulling, by Hurle *et al.* [1974] who exhibited oscillatory regimes in molten gallium and determined the critical values (denoted $Gr_{c,\,osc}$) of the Grashof number, Gr, for the

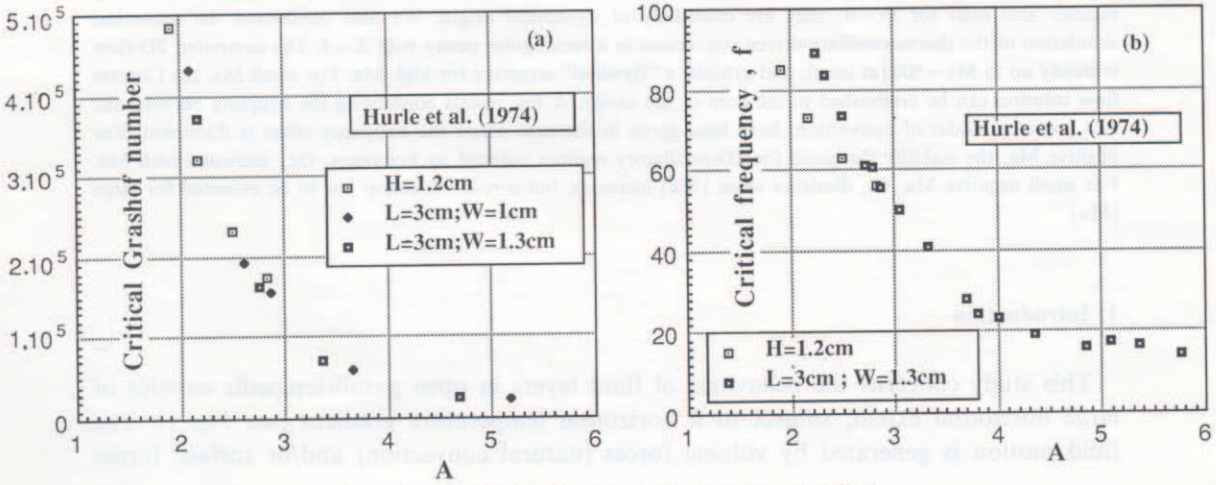

Fig. 2. —Critical conditions *vs* A, after Hurle *et al.* [1974]; (*a*) $Gr_{c,\,osc}$; (*b*) frequency.

onset of oscillations. $Gr_{c,\,osc}$ values are plotted in terms of the aspect ratio A, in Figure 2*a* and the corresponding frequencies, in Figure 2*b*. The study of Hurle *et al.* [1974] would tend to indicate that oscillations observed by previous authors during directional solidification (with a given pulling rate), came from the melt. Several reviews of such melt oscillation have been proposed, [Carruthers, 1974], [Pimpukar & Ostrach, 1981], [Polezhaev, 1984], [Ben Hadid & Roux, 1986], [Ben Hadid *et al.*, 1986], [Winters, 1987, 1988].

Some theoretical attempts at explaining the origin of the experimental melt oscillations have been made, by Gill [1974] and Hart [1983] who performed a small perturbation analysis of a steady unidirectional basic flow (Hadley circulation; Hart [1972]), existing for large cavities in the direction of the external temperature gradient. As yet, these studies have not supplied the expected explanation.

An accurate localisation of the oscillatory instability has been proposed by Winters [1987, 1988], who looks for a Hopf bifurcation in the solution of steady natural-convection equations, on the basis of a continuation method. This study, for two-dimensional cases, gives the variation of the critical Grashof number in terms of the Prandtl number, in the range $0 \leqq Pr \leqq 0.05$, for a cavity of aspect ratio (lenth/height) equal to 4.

In the case where only the thermocapillary convection plays a role, typically for very thin layers, Smith & Davis [1983] showed the possible existence of thermal oscillations, by performing a small perturbation analysis of a steady unidirectional basic flow (of Couette type), also generated by the thermocapillarity in the direction of the external temperature gradient.

The aim of the present paper is to present a new analysis of the melt-oscillation problem, taking into account recent results by Laure & Roux [1987] concerning the stability analysis of the basic flow (Hadley circulation) previously considered [H., 1983], and the results of direct numerical simulation of natural convection equations [B. H. & R., 1986], in the case of rectangular cavities (see *Fig.* 3).

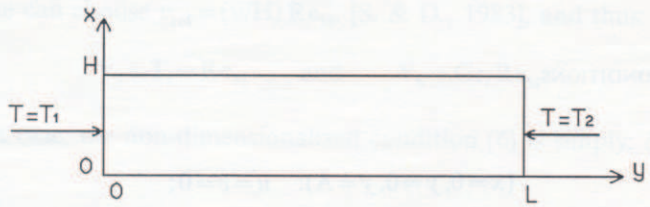

Fig. 3. — Two-dimensional model.

2. Formulation of the problem

We consider an open rectangular cavity, bounded by two vertical isothermal walls (with temperatures T_1 et T_2), and filled with a low-Prandtl-number fluid. As soon as $T_1 \neq T_2$, a convective motion occurs due to the horizontal temperature gradient. Such a motion is dominated by the thermocapillary convection in the case of thin layers (less than a few millimeters); in this case the motion intensity is characterized by the Marangoni number defined as $\mathbf{Ma} = -\partial\sigma/\partial T \; G_h H^2/(\rho\nu\kappa)$, where H is taken as the reference length and where $G_h = \Delta T/L$, with $\Delta T = T_1 - T_2$. H and L represent, respectively, the height and the length of the cavity, and A its aspect ratio: $\mathbf{A} = L/H$. We will also use the Reynolds-Marangoni number, defined by $Re_M = Ma/Pr$. In the case of natural convection, the motion intensity is characterized by the Grashof number, $Gr = g\beta G_h H^4/\nu^2$, which is based on the height of the cavity.

2.1. Governing equations: (two-dimensional case)

The model used here is essentially based on the two-dimensional Navier-Stokes equations coupled to the energy transport equation. In this study we shall assume that the

velocity is small enough to consider the flow as laminar. Also, the fluid is assumed to satisfy the Boussinesq approximation, and thus it is considered as quasi-incompressible.

With the notation proposed by de Vahl Davis [1986], the Navier-Stokes equations can be written in the ψ and Ω formulation (streamfunction and vorticity), as

$$\Omega_t + \mathbf{V_i}[u\,\Omega_x + v\,\Omega_y] = \mathbf{V_d}[\Omega_{xx} + \Omega_{yy}] - \mathbf{V_b}\,\theta_y \tag{1}$$

$$\psi_{xx} + \psi_{yy} + \Omega = 0 \tag{2}$$

with:

$$u = \psi_y\,; \qquad v = -\psi_x \qquad \text{and} \qquad \Omega = v_x - u_y. \tag{3}$$

The energy transport equation writes

$$\theta_t + \mathbf{T_i}[u\,\theta_x + v\,\theta_y] = \mathbf{T_d}[\theta_{xx} + \theta_{yy}] \tag{4}$$

where:

$$\theta = (T - T_2)/T_{ref} \qquad \text{with} \quad T_{ref} = (T_1 - T_2)/A.$$

2.2. Boundary conditions

On rigid walls

$$(x = 0, y = 0, y = A): \quad u = v = 0\,; \tag{5}$$

– on the upper surface ($x = 1$) which is assumed planar, one has: $u = 0$, and after Birikh [1966 *b*], the equilibrium condition is written as:

$$\mu\, v_{ref}\, \partial v/\partial x = (\partial\sigma/\partial T)\, T_{ref}\, (\partial\theta/\partial y), \tag{6}$$

where v_{ref} and T_{ref} are reference quantities;

– on the isothermal vertical walls, one has:

$$\theta_{(x,\,0)} = \theta_1 = A\,; \qquad \theta_{(x,\,A)} = \theta_2 = 0\,; \tag{7}$$

while on the horizontal surfaces, one considers the two following types of thermal conditions:

$$\theta_x = 0 \quad \text{(adiabatic surface)} \tag{8 a}$$

or

$$\theta = A - y \quad \text{(perfectly "conducting" surface).} \tag{8 b}$$

2.3. Nondimensionalization

Taking $t_{ref} = H^2/\nu$ as the time scale, one has:

$$\mathbf{V_d} = 1\,; \qquad \mathbf{T_d} = 1/Pr\,; \qquad \mathbf{V_i} = \mathbf{T_i} = v_{ref}\, H/\nu \quad \text{and} \quad \mathbf{V_b} = g\,\beta\, H^2/(\nu\, v_{ref}). \tag{9}$$

Thus, depending on the selected reference velocity, v_{ref}, different types of nondimensionalization will be considered:

– for small Gr (equilibrium between buoyancy and viscosity terms), one can take after Hart [1983]:

$v_{ref}=(\nu/H)\,Gr$ and thus:

$$\mathbf{V_i}=\mathbf{T_i}=Gr \quad \text{and} \quad \mathbf{V_b}=1 \tag{9a}$$

– for large Gr (equilibrium between buoyancy and inertial terms), one can take after Ostrach [1976]:

$$v_{ref}=(\nu/H)\,Gr^{0.5}$$

and thus:

$$\mathbf{V_i}=\mathbf{T_i}=Gr^{0.5} \quad \text{and} \quad \mathbf{V_b}=Gr^{0.5} \tag{9b}$$

– if thermocapillary convection dominates natural convection, and if inertial terms remain small, one can choose $v_{ref}=(\nu/H)\,Re_M$, [S. & D., 1983], and thus:

$$\mathbf{V_i}=\mathbf{T_i}=Re_M \quad \text{and} \quad \mathbf{V_b}=Gr/Re_M. \tag{9c}$$

Note that, in this case, the non-dimensionalized condition (6) is simply: $\partial v/\partial x=-\partial\theta/\partial y$.

2.4. Limiting case $Pr=0$

In the limiting case $Pr=0$ (ν finite and κ infinite), Eq. (4) reduces to $\theta_{xx}+\theta_{yy}=0$ and its solution, accounting for the conditions (7) and (8) is simply:

$$\theta=A-y. \tag{10}$$

The resulting equations correspond to the Navier-Stokes equations with a constant source term, as $\theta_y=-1$:

$$\Omega_t+\mathbf{V_i}[u\,\Omega_x+v\,\Omega_y]=\mathbf{V_d}[\Omega_{xx}+\Omega_{yy}]+\mathbf{V_b}. \tag{11}$$

2.5. Cavity of infinite extent, A $z\to\infty$ (Birikh's solution)

In the case of cavity of infinite extent (finite H and $L\gg H$), a steady solution exists for small temperature differences $\Delta T=T_1-T_2$. This solution corresponds to unidirectional flow in the y-direction, with $u=0$ and $v=v(x)$. In the case of natural convection, this solution, which will be denoted $v_{R-F}(x)$, has been exhibited [B., 1966 *a*]; it is also known as Hadley circulation, after the work of Hart [1972] on the physics of the atmosphere. In the case of Marangoni convection, the profile $v=v_M(x)$ corresponds to a Couette type solution; the associated temperature profiles have been given [B., 1966 *b*]. This solution can be expressed in the different cases by writting the mass flow

rate conservation in the vertical plane $\left(\int_0^1 v\,dx=0\right)$ and the conditions (5) and (6), by:

$$v_{R-F}(x)=\theta_y(8x^2-15x+6)x/48=-(8x^2-15x+6)x/48 \tag{12}$$

$$v_M(x)=-\theta_y(3x-2)x/4=(3x-2)x/4. \tag{13}$$

Note that in expression (12) $v_{R-F}(x)$ is scaled with (ν/H) Gr, and that in expression (13) $v_M(x)$ is scaled with (ν/H) Re_M. The surface velocities are: $v_{R-F}(1)=1/48$ and $v_M(1)=1/4$. In the coupled case, these two velocities add when $Re_M>0$; which corresponds to the more classical case ($\partial\sigma/\partial T<0$).

A vertical temperature profile, $T(x)$, such that $\theta(x, y)=T(x)+A-y$ can be associated with $v(x)$. It is simply obtained from (4) by integrating $T_{xx}=\mathbf{T_i}/\mathbf{T_d}\,v\,\theta_y$, with the boundary conditions (8).

3. Small perturbation stability (natural convection alone)

To study the behaviour of small perturbations of the velocity vector $u(u, v, w)$, temperature θ, and pressure q, we use the Navier-Stokes equations with primitive variables, which can be written after linearisation as:

$$\frac{\partial u}{\partial t}+\mathrm{Gr}(U_0.\nabla u+u.\nabla U_0)=-\nabla q+\theta e_x+\Delta u \tag{14}$$

$$\frac{\partial \theta}{\partial t}+\mathrm{Gr}(U_0.\nabla \theta+u.\nabla T_0)=\frac{\Delta u}{\mathrm{Pr}} \tag{15}$$

where U_0 is the vector (0, $v(x)$, 0) representing the basic flow.

In the y- and z-directions, the boundary conditions are replaced by periodicity conditions. Thus, to obtain the neutral stability curve, one seeks solutions of the perturbation equations of the form:

$$u(x, y, z)=\mathbf{u}(x)\,e^{i(hy+kz)+\lambda t}, \tag{16}$$

$$q(x, y, z)=\mathbf{q}(x)\,e^{i(hy+kz)+\lambda t}, \tag{17}$$

$$\theta(x, y, z)=\theta(x)\,e^{i(hy+kz)+\lambda t}. \tag{18}$$

In these expressions (16-18), the wavenumbers h and k are real, while λ is complex:

$\lambda=\lambda_r+i\lambda_i$. In the following, we will also use the associated wavelengths $\lambda_y=2\pi/h$ and $\lambda_z=2\pi/k$, scaled with H, and the frequency, $f=\lambda_i/2\pi$, scaled with ν/H^2.

By substituting for (u, q, θ) from expressions (16-18) in the linearized system (14-15), one obtains a differential system of the form:

$$L_{hk}\,\mathbf{W}=\lambda\,\mathbf{W}; \tag{19}$$

with $\mathbf{W}=(\mathbf{u}(x), \theta(x))$ and L_{hk} depending on Pr and Gr.

This equation is solved by a Tau method, using Chebychev polynomials as basis functions. The efficiency of such a technique, for natural convection equations, has been demonstrated in a preceding paper [Brenier *et al.*, 1986].

Accounting for the symmetries of the problem, Laure [1987] showed that the critical Grashof number, Gr_c, can be obtained for solutions with the form $(h, 0)$ or $(0, k)$. It is thus necessary to verify if solutions of this type are local extrema. We recall that Gr_c is defined by

$$Gr_c = \inf_{h,\, k \in \mathcal{R}} Gr_0(Pr, h, k) \tag{20}$$

where Gr_0 is the value of Gr such that the largest eigenvalue of the linear operator L_{hk} is purely imaginary (eventually null: monotonic case).

First, we verified the existence of a neutral stability curve, of 3D oscillatory type, predicted by Hart [1983]. The results are presented in Figure 4. A non-linear stability

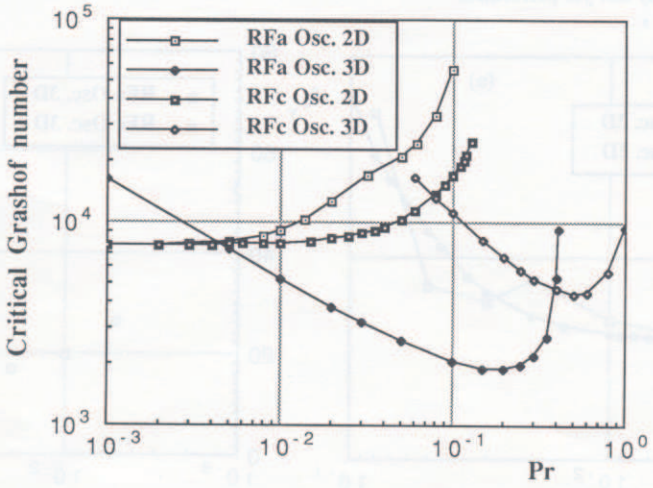

Fig. 4. — Gr_c *vs* Pr, after Laure & Roux [1987].

analysis performed by Laure [1987] shows that the 3D oscillatory solutions stable beyond the bifurcation point and takes the form of a travelling plane wave for $0.004\,5 \leqq Pr \leqq 0.38$, and of a stationary wave for $0.38 \leqq Pr \leqq 0.41$ (*see* Table I).

More recently, Laure & Roux [1987] showed the existence a 2D oscillatory mode; the neutral stability curves corresponding to adiabatic and conducting conditions are also plotted in Figure 4. This figure shows that this 2D mode is the first to occur, in the range $0 \leqq Pr \leqq 0.004\,5$ for the adiabatic case, and in the range $0 \leqq Pr \leqq 0.077$ for the conducting case. These two neutral stability curves asymptotically tend to a unique limit, $Gr_c = 7{,}580$, when $Pr \to 0$. The critical spatial period, λ_y (based on H), is presented in Figure 5 *a*. It only weakly depends on the thermal boundary conditions and is practically independent of Pr in the range $0 \leqq Pr \leqq 0.03$ ($\lambda_y \approx 4{,}6$ at $Pr = 0$).

In the case of 3D oscillations, the behavior is completely different (*Fig.* 5 *b*); λ_y tends to infinity for $Pr \approx 0.15$. We also present in Figure 6, the behavior of the critical wavelength, λ_z, in z-direction. We observe a very large difference between the solution

TABLE I. — Stability results; characteristics of the bifurcated solutions.

Therm. Cond.		Bifurcation Type
Adiabatic	$0.001 \leqq Pr \leqq 0.004\,5$	2D Oscillatory flow (*) $\lambda_y \approx 4.6$; $f \approx 9$
	$0.004\,5 \leqq Pr \leqq 0.38$	3D stable Oscillatory flow $\lambda_y \approx 10\lambda_z$; $9 \leqq \lambda_z \leqq 32$; $f \approx 2.5$ Travelling plane wave
	$0.38 \leqq Pr \leqq 0.41$	3D stable Oscillatory flow $\lambda_y \approx 10\lambda_z$; $\lambda_z \approx 16$; $f \approx 2.5$ Stationary plane wave
Conducting	$0.001 \leqq Pr \leqq 0.077$	2D Oscillatory flow (*) $\lambda_y \approx 4.6$; $f \approx 9$
	$0.077 \leqq Pr \leqq 1$	3D Oscillatory flow (*) $\lambda_y \approx 10\lambda_z$; $\lambda_z \approx 3.7$; $9.5 \leqq f \leqq 18.5$

(*) Non-linear study not yet performed.

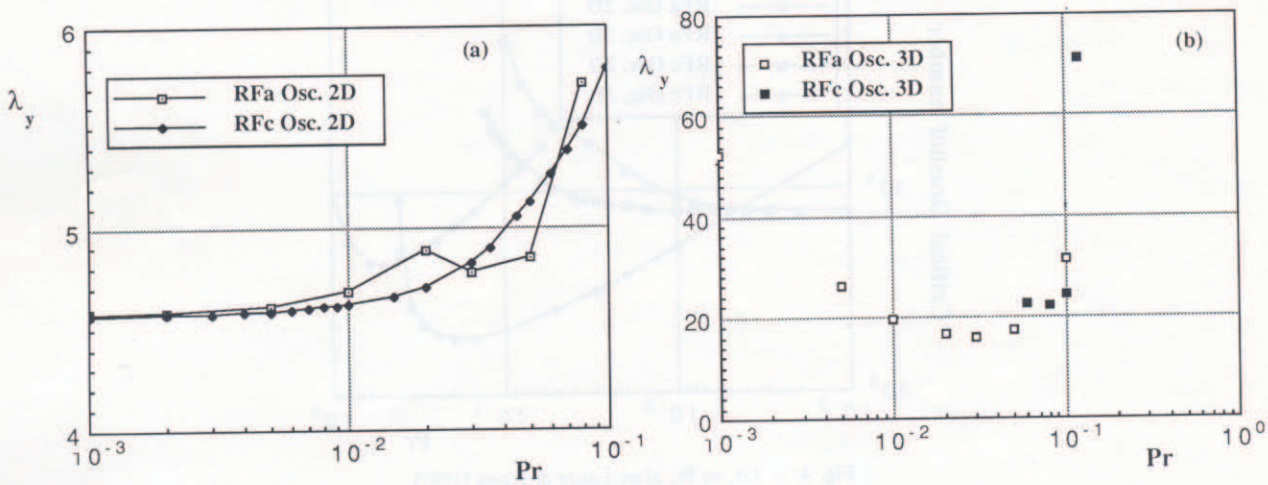

Fig. 5. — λ_y *vs* Pr, after Laure & Roux [1987]; (*a*) 2D-case; (*b*) 3D-case.

corresponding to the adiabatic case for which λ_z tends to infinity when $Pr \to 0$, and the one corresponding to the conducting case where λ_z keeps moderate values, close to 4, for the range $0.05 \leqq Pr \leqq 0.5$.

The real existence of 2D oscillatory disturbances (*i. e.* the solution stability beyonds the bifurcation point) could be studied by means of the non-linear stability theory of Laure [1987]. But it has already been proved by the results of the computation of the 2D governing equations, as shown in a paper by Ben Hadid *et al.*, [1986], the main results of which are summarized here. In addition, the trend of the 2D neutral stability curves (*Fig.* 4), are in excellent agreement with the results recently obtained [W., 1987, 1988] in the case of a confined layer ($A = 4$). These results which are presented in Figure 7 *a*, have been obtained by analysing the stability of 2D steady numerical solutions, obtained by a direct simulation [Winters *et al.*, 1987]. Of course, the critical values obtained by Winters are higher ($Gr_c = 13{,}750$ for $Pr = 0$), due to the confinement effect

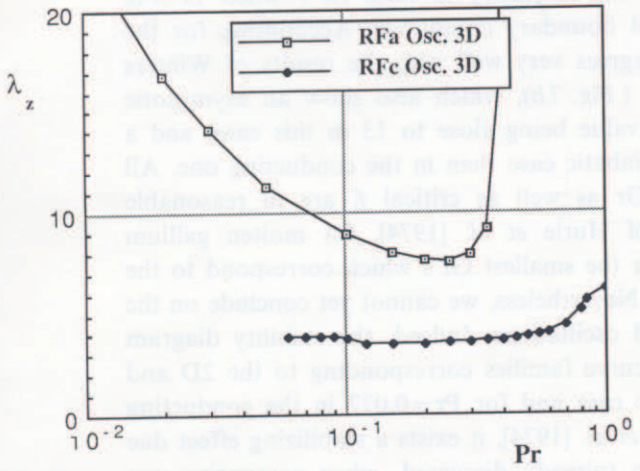

Fig. 6. — λ_z *vs* Pr, after Laure & Roux [1987].

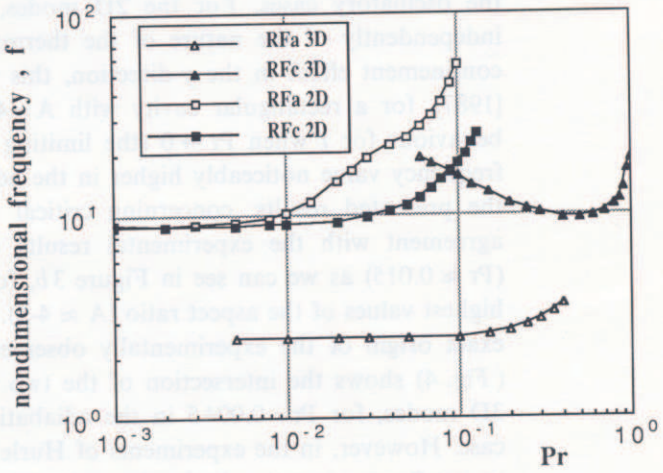

Fig. 8. — Frequency *vs* Pr, after Laure & Roux [1987].

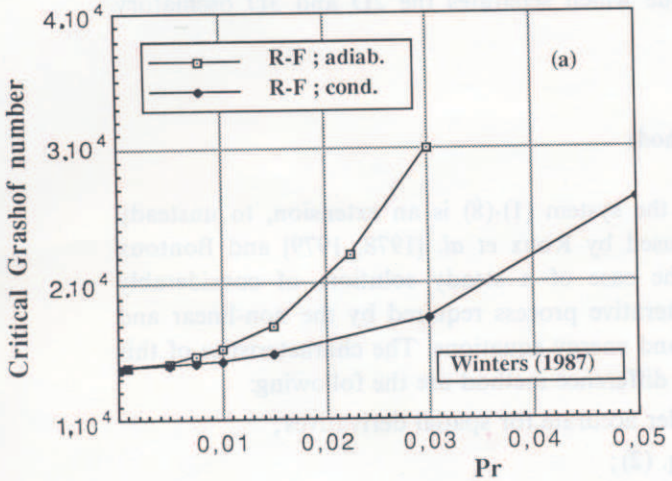

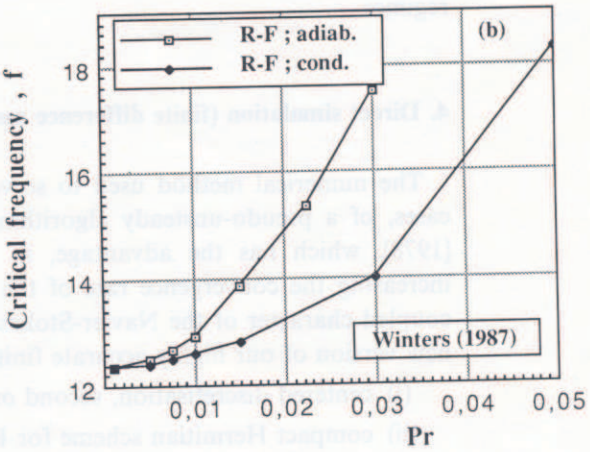

Fig. 7. — Critical conditions *vs* Pr, after Winters [1987]; (*a*) $Gr_{c,osc}$; (*b*) frequency.

in the y-direction, but we recover all the main characteristics of Figure 4, with, in particular: the same asymptotic behaviour of the neutral stability curves when $Pr \to 0$, and the same relative position of the neutral stability curves corresponding to adiabatic and conducting cases, respectively ($Gr_{c,\,cond} < Gr_{c,\,adiab}$).

The frequency f (non-dimensionalized by $t_{ref}^{-1} = \nu/H^2$) is presented in Figure 8 for all the oscillatory cases. For the 2D modes, the frequency is close to 9 when $Pr \to 0$, independently of the nature of the thermal boundary conditions. Accounting for the confinement effect in the y-direction, this agrees very well with the results of Winters [1987], for a rectangular cavity with $A = 4$ (*Fig.* 7*b*), which also show an asymptotic behaviour for f when $Pr \to 0$ (the limiting value being close to 13 in this case) and a frequency value noticeably higher in the adiabatic case than in the conducting one. All the presented results, concerning critical Gr as well as critical f, are in reasonable agreement with the experimental results of Hurle *et al.* [1974], for molten gallium ($Pr \approx 0.015$) as we can see in Figure 3*b*, for the smallest Gr's which correspond to the highest values of the aspect ratio ($A \approx 4$-5). Nevertheless, we cannot yet conclude on the exact origin of the experimentally observed oscillations. Indeed, the stability diagram (*Fig.* 4) shows the intersection of the two curve families corresponding to the 2D and 3D modes, for $Pr = 0.004\,5$ in the adiabatic case and for $Pr = 0.077$ in the conducting case. However, in the experiments of Hurle *et al.* [1974], it exists a stabilizing effect due to confinement not only in the y-direction (already discussed, when comparing our stability results for infinite layer and those of Winters [1987] for $A = 4$), but also in the z-direction (as $W \approx H$). Thus, all the stability curves (and mainly the ones corresponding to 3D regimes) will be shifted upward to positive Gr's, in different ways. This shifting, which is difficult to quantify (as the critical spatial periods of the 3D modes are also greatly influenced by the thermal boundary conditions), will be associated with a substantial increase in the Prandtl number value which separates the 2D and 3D oscillatory regimes.

4. Direct simulation (finite difference method)

The numerical method used to solve the system (1)-(8) is an extension, to unsteady cases, of a pseudo-unsteady algorithm used by Roux *et al.* [1978, 1979] and Bontoux [1978], which has the advantage, in the case of a steady solution, of considerably increasing the convergence rate of the iterative process required by the non-linear and coupled character of the Navier-Stokes and energy equations. The characteristics of this new version of our highly accurate finite difference method are the following:

(i) centered discretisation, second order accurate for spatial derivatives;

(ii) compact Hermitian scheme for Eq. (2);

(iii) second order accurate approximation for the boundary conditions on the vorticity;

(iv) an alternate direction implicit (ADI) method to solve the transport equations (1) and (4); this method includes a compatibility condition on the boundary at the intermediate time step [Fairweather & Mitchell, 1967], and an iterative process at each time step;

(v) internal iterations, needed to adjust ψ values in Eq. (2).

5. Results and discussion

5.1. Natural convection alone

The computations have been carried out with the unsteady version of the code, in the case of a rectangular cavity with $A=4$. The oscillatory regimes have been mainly characterized by the time history of the maximum of the streamfunction, ψ_{max}. When the numerical solution presents ψ_{max} oscillations, these oscillations are followed for several tens of periods, in order to check their stability. It is always difficult to accurately determine the threshold for the onset of the oscillatory regime, as the damping rate (and the oscillation amplitude) decreases when this threshold is approached. In addition, some numerical tests showed that spurious oscillations can exist if the internal iterations on ψ are stopped too soon by using a weak convergence criteria. The choice of the discretisation step size also plays an important role; most of the computations have been performed using a grid of 31×61 points until $Gr=10^4$ and with a grid of 37×85 points, for higher Gr [B. H. & R., 1986]. When approaching the onset of oscillations, a very fine grid is needed and we finally used up to 41×121 grid points.

In the limiting case $Pr=0$, the threshold is found near $Gr=1.5\times10^4$. The ψ_{max} fluctuations are damped for this last value, but not for $Gr=1.375\times10^4$ (fluctuations remaining of the order of 0.8%) with a non-dimensionalized frequency of $f=12.25$. This critical Gr value is very close to the threshold predicted by Winters [1987], *i. e.* 1.375×10^4. The fluctuation amplitude and frequency are noticeably increasing with Gr, in the range

TABLE II. — Characteristics of the flow in terms of Gr, R-F case at $Pr=0$.

Gr	ψ_{max}	ψ-fluct. (%)	f	Regimes
1.0×10^4	0.555	–	–	Steady state
1.35×10^4	0.609	0.6	12.25	+
1.375×10^4	0.612 (*)	0.8	12.42	Oscillatory
1.4×10^4	0.613 (*)	4.5	12.65	Oscillatory
1.5×10^4	0.617 (*)	8.9	13.24	Oscillatory
2.0×10^4	0.636 (*)	17.5	16.18	Oscillatory
3.0×10^4	0.680 (*)	20.9	23.21	Oscillatory

(*) Mean value over a period.

$1.375\times10^4\leqq Gr\leqq3\times10^4$ (*see* Table II). Note that our preliminary results (B. H. & R., 1986], with a grid of 31×61 points were again not accurate enough.

For $Pr=0.015$, computations have been performed in the case of a conducting free-surface. Fluctuations of ψ_{max} are damped for $Gr\leqq1.475\times10^4$, but they are maintained (with small-amplitude, close to 2.4%) for $Gr=1.5\times10^4$. The threshold value again corresponds well to the one predicted by Winters [1987]. Some characteristics of the flow

TABLE III. — Characteristics of the flow in terms of Gr, R-Fc case at Pr = 0.015.

Gr	ψ_{max}	ψ-fluct. (%)	f	Regimes
1.0×10^4	0.553	–	–	Steady state
1.475×10^4	0.617 (*)	–	–	+
1.5×10^4	0.619 (*)	2.4	12.94	Oscillatory
2.0×10^4	0.635 (*)	15.9	15.92	Oscillatory
3.0×10^4	0.668 (*)	19.3	20.90	Oscillatory

(*) Mean value over a period.

are given for $1 \times 10^4 \leqq Gr \leqq 3 \times 10^4$, in Table III. The frequency is again observed to increase with Gr. At $Gr = 3 \times 10^4$, this frequency equals 20.9, and is very close to the one calculated for Pr = 0.

For $Gr = 8 \times 10^4$, the flow oscillates with the frequency $f = 42$. This Gr value corresponds to a case treated by Crochet *et al.*, [1983], and interpreted by these authors as the beginning of the oscillatory regime (*see* their Figure 4, where Ra = 4,750, in their notation). The present code predicts the onset of oscillations for Gr values noticeably smaller than the ones predicted [C. *et al.* 1983]. This discrepancy is certainly due, as we have seen for our own results, to the grid used by these authors not being fine enough. Nevertheless, we observed, for a higher value of Gr ($Gr = 1.6 \times 10^5$) and also considered by Crochet *et al.* [1983] (*see* their Figure 6, where $Ra = 10^5$ in their notation), a very

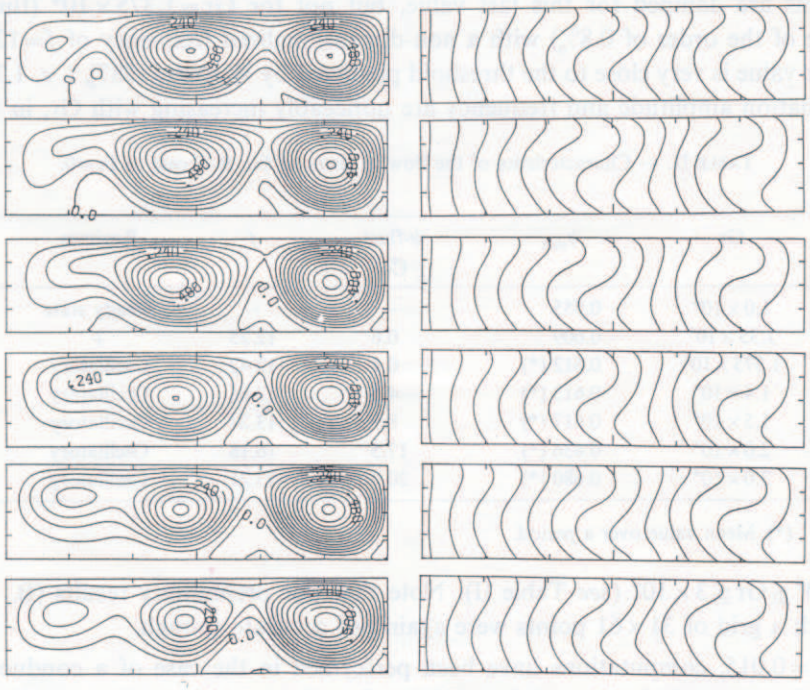

Fig. 9. — Evolution of the flow structure, at six regular intervals over one period, for $Gr = 1.6 \times 10^5$ and Pr = 0.015. (*a*) streamfunctions; (*b*) isotherms.

similar evolution of the streamlines and isotherms (*Fig.* 9 *a* et *b* respectively), plotted for a few regularly-spaced instants over a period. This certainly means that, far from the bifurcation point, the sensitivity of the numerical solution diminishes.

One can conclude that 2D-oscillatory modes exist for small Pr. These oscillations certainly have a dynamical origin as they are also found for $Pr=0$, and the threshold for the onset of these modes is probably connected to a critical speed in the melt (that we would have to calculate!). This speed is reached for a minimum value of Gr at $Pr=0$, and for higher Gr when Pr increases (leading to more viscous damping). One can consider that in the adiabatic case, the thermal stratification (stabilizing) which occurs when Gr increases, is more pronounced than for the conducting case (giving an increased damping of the flow); this could explain the relative position of the neutral stability curves ($Gr_{c,\,cond} < Gr_{c,\,adiab}$) in Figure 4, in the 2D case. For a cavity of large extent, this stratification can be characterized by the maximum value of the vertical temperature gradient that we will denote G_v. This maximum is reached at the point where $(\partial^2\theta/\partial x^2)=0$; *i. e.* at the point where $v=0$. The expressions of $G_v=(\partial\theta/\partial x)_{v=0}$, in the

TABLE IV. — Maximum positive thermal stratification, $(\partial\theta/\partial x)_{v=0}$; 1 D steady basic flow ($A \to \infty$).

Case	Position of the point of zero velocity	Maximum thermal stratification $G_v=(\partial\theta/\partial x)_{v=0}$
R-F adiabatic.	$x=0.578\,5$	$G_v=0.541\,6\times10^{-2}$ Gr Pr
R-F conducting.	$x=0.578\,5$	$G_v=0.229\,1\times10^{-2}$ Gr Pr
M adiabatic.	$x=2/3$	$G_v=0.370\,4\times10^{-1}$ Ma
M conducting.	$x=2/3$	$G_v=0.162\,1\times10^{-1}$ Ma

conducting and adiabatic cases, are given in Table IV, where the values corresponding to thermocapillary convection are also included. The maximum of thermal stratification is nearly twice as great in the adiabatic case as in the conducting one. One can remark that G_v is proportional to the Rayleigh number ($Ra=Gr\,Pr$) for natural convection, and to $Ma=Re_M\,Pr$ in the case of thermocapillary convection.

5.2. THERMOCAPILLARY CONVECTION ALONE

We now consider the case where thermocapillary convection dominates, for the two extreme cases where the free-surface is either conducting or adiabatic. For a conducting free-surface, the shear-stress is constant and independent of the temperature field in the fluid; the energy equation (4) being uncoupled from the Navier-Stokes Eq. (1).

A stability analysis of the Couette flow solution (13) associated with a constant thermocapillary force in the y-direction (case of infinitely extended cavity in the y-direction), has been developed [S. & D., 1983]. This study showed oscillatory instabilities occurring, for small Pr, as "hydrothermic" waves propagating obliquely (in the plane Oy, Oz), with angles $+\Phi$ et $-\Phi$ with respect to the basic flow (in the y-direction). This angle Φ is close to 75° when $Pr \to 0$. The flow structure beyond this bifurcation point would be essentially 3D. The neutral stability curves have been given [S. & D., 1983] in the case of an adiabatic upper surface (*see* their Figs. 17 to 20). These authors stated

that for finite Biot numbers, the fluid layer is always more stable than for the adiabatic case (Bi = 0). The critical Marangoni number, Ma_c, for the beginning of the oscillatory regime is close to 2 for Pr = 0.001 and varies as $Pr^{1/2}$, when Pr → 0 (see *Fig.* 17 of Smith & Davis); thus, the critical value of Re_M increases as $Pr^{-1/2}$, when Pr → 0. For Pr = 0.015 for example, oscillations occur for Ma = 9, *i. e.* for $Re_M = 600$. The frequency of these oscillations (always based on ν/H^2) is nearly 2.4 (see *Fig.* 20 of Smith & Davis), *i. e.* noticeably smaller than for natural convection alone. But, we have to note that the propagation directions of the perturbations are at angles $\Phi = \pm 77°$ with O*y*, and that the critical wavelength in the *z*-direction, λ_z (based on H), which varies as $2.6\ Pr^{-1/2}$, is equal to 19 (see *Figs.* 18 and 19 of Smith & Davis). Thus, these oscillations can only be observed in very wide cavities (W ≫ H).

In fact, experiments performed by Camel *et al.* [1986], in cavities which don't have such a width condition, don't present oscillations even for high Re_M ($Re_M \approx 10^4$). This could indicate that either the confinement exerted by the lateral walls at $z = \pm W$ produces an important damping, or that the basic flow never reaches the fully-developed regime and thus contains a stabilizing effect due to inertial terms with an accelerating flow in most parts of the cavity.

Computations are carried out for Pr = 0.015 and for a wide range of Ma, from 1 (below the stability threshold given by Smith & Davis), up to 500. The results concerning streamlines and isotherms are presented in Figures 10 *a* and *b*, for the conducting case, and in Figures 11 *a* and *b*, for the adiabatic case. In this range of Ma, no oscillations occurred. Of course, this is not in contradiction with the stability results of Smith & Davis [1983], as our numerical model is limited to the 2D case, in the plane (O*x*, O*y*). Computations have been performed with a grid of 35×95 nodes, with a node stretching near the vertical walls (such that $\Delta x_{min} \approx 0.012$ H). This grid ensures a good accuracy for the velocity (better than 1 %) up to Ma = 500.

The absence of oscillations in the 2D numerical solutions is also confirmed by the results given by other authors, e.g. Polezhaev *et al.* [1981] for Pr = 1, A = 1 and 2, and for $Ma = 10^2$, 10^3 and 10^4; Wilke & Löser [1983] for liquid silicium (Pr = 0.026), for A = 1 and Ma = 700 ($Re_M = 2.7 \times 10^4$); and Zebib *et al.* [1985] for A = 1, Pr = 0.1 and $10^3 \leqq Re_M \leqq 5 \times 10^4$. Wilke & Löser [1983] also obtained a steady solution even for $Ma = 7 \times 10^3$ ($Re_M = 2.7 \times 10^5$), but in this case the flow is multi-cellular.

The results presented in Figures 10 and 11 correspond to positive Marangoni numbers; in this case, the liquid along the liquid-gas interface is flowing from a hot wall to a cold end wall. The computed flows present a structure with a concentrated vortex, near the cold wall. This tendency (center of the vortex near the cold wall for small Pr), is also mentioned in previous papers [W. & L., 1983]; [Z. *et al.*, 1985] for a square cavity (A = 1). Zebib *et al.* [1985] results show that this tendency only exists for moderate Re_M ($Re_M = 10^3$); while for higher Reynolds-Marangoni numbers, $10^4 \leqq Re_M \leqq 5 \times 10^4$, on the contrary, the flow structure is close to the one corresponding to Pr = 1, with a vortex centered near the median plane, $y = L/2$. Evidently, the similarity of the behaviour observed [Z. *et al.*, 1985] for different Pr, when the Marangoni number (product of Re_M by Pr) is large enough ($10^3 \leqq Ma \leqq 5 \times 10^3$), is due to the similarity of the temperature

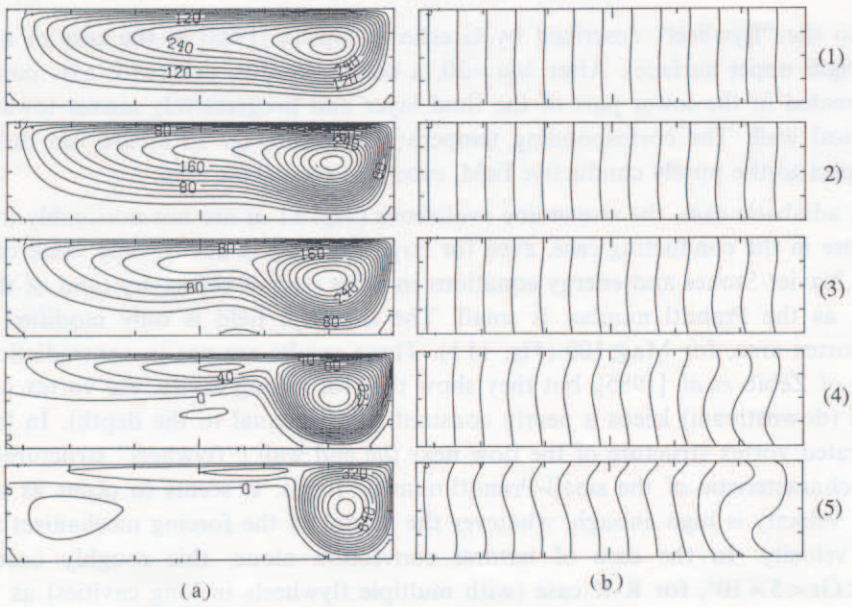

Fig. 10. – Influence of the Marangoni number on the flow structure, in the conducting case, for Pr = 0.015: (1) Ma = 5; (2) Ma = 10; (3) Ma = 20; (4) Ma = 100; (5) Ma = 500. (*a*) streamfunctions; (*b*) isotherms.

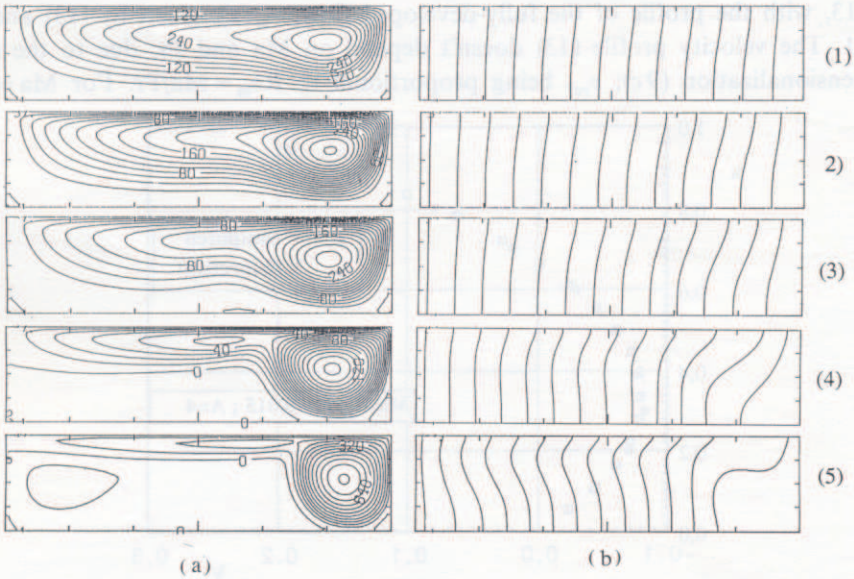

Fig. 11. – Influence of the Marangoni number on the flow structure, in the adiabatic case, for Pr = 0.015: (1) Ma = 5; (2) Ma = 10; (3) Ma = 20; (4) Ma = 100; (5) Ma = 500. (*a*) streamfunctions; (*b*) isotherms.

profile along the free-surface, which presents in this case a plateau on most of the layer, leading to a strong reduction in the thermocapillary forces on this interface.

On the contrary, our results for Pr = 0.015 show the formation of a more and more concentrated vortex when Ma increases (Ma = 5, 10; 20; 100; 500), in the conducting case (*Fig.* 10 *a*) as well as in the adiabatic one (*Fig.* 11 *a*). This vortex structure is very

similar to the "flywheel" described by Gresho & Upson [1983] in the case of a closed cavity (rigid upper surface). After Ma = 20, a contra-rotative cell (with axis parallel to Oz) is created in the lower part of the fluid layer and progressively moves towards the hot vertical wall. The corresponding temperature fields (*Fig.* 10 *b*) are not deformed, with respect to the purely conductive field, except in the vortex area.

In the adiabatic case, the streamline evolutions (*Fig.* 11 *a*) are not noticeably different from those in the conducting case, even for large Ma; this is due to only weak coupling between Navier-Stokes and energy equations in most part of the cavity (and of the free-surface), as the Prandtl number is small. The isotherm field is only modified in the strong vortex area, for $Ma \geqq 100$ (*Fig.* 11 *b*). These results are not in contradiction with the ones of Zebib *et al.* [1985], but they show that for a long cavity, the vortex near the end wall (downstream) keeps a nearly constant length (equal to the depth). In fact this concentrated vortex structure of the flow near the end wall ("flywheel" structure) seems to be a characteristic of the small-Prandtl-number fluids. It seems to occur as soon as the flow velocity is high enough, whatever the nature of the forcing mechanism leading to this velocity. In the case of natural convection alone, this roughly occurs for $2 \times 10^4 < Gr < 5 \times 10^4$, for R-R case (with multiple flywheels in long cavities) as well as for R-F case ([B. H. *et al.*, 1986]; [C. *et al.*, 1983], for example).

The velocity profiles $v(x)$ in the median plane ($y = A/2$) have been compared in Figures 12 and 13, with the profile of the fully-developed flow, $v_M(x)$, given by (13) and valid for $A \gg 1$. The velocity profile (13) doesn't depend on Ma and Pr, due to the chosen non-dimensionalization (9 *c*); v_{ref} being proportional to $Re_M = Ma/Pr$. For Ma = 1, the

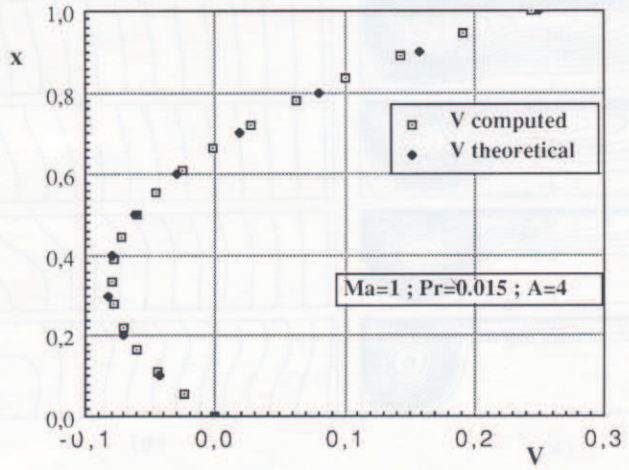

Fig. 12. – Velocity profile, $v(x)$, at $y = A/2$; Ma = 1.

agreement between $v(x)$ and $v_M(x)$ is excellent (*Fig.* 12), but the profile $v(x)$ rapidly differs from $v_M(x)$ when Ma is increased (*Fig.* 13), for a given A; in particular, the absolute value of the surface velocity rapidly diminishes from the (maximum) asymptotic value, 0.25, indicating either a confinement effect or a regime change.

The longitudinal evolution of the surface velocity for $0 \leqq y/A \leqq 0.5$ is presented in Figure 14, for different Ma. These curves show that the surface flow is accelerated on

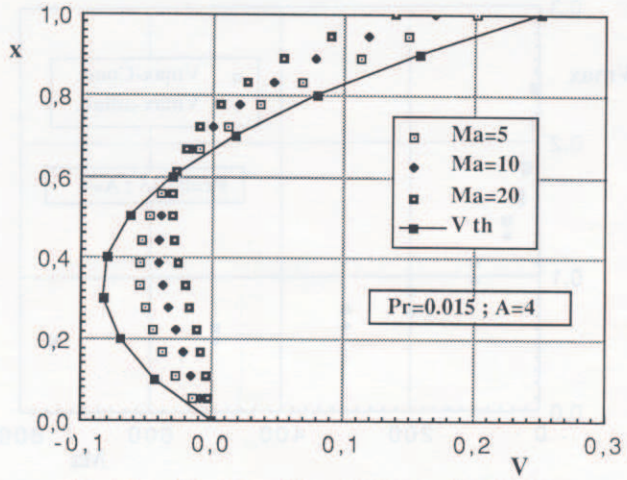

Fig. 13. — Velocity profiles, $v(x)$, at $y = A/2$; $Ma \geqq 5$.

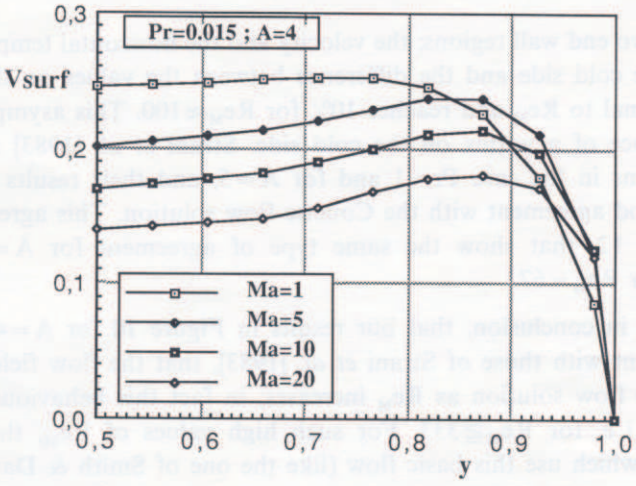

Fig. 14. — Longitudinal variation of the velocity, at the free-surface.

the major part of the layer and only reaches the asymptotic (Couette flow) limit for $Ma \approx 1$; in all other cases, the fluid layer is subject to a deceleration due to the endwall ($y = 0$) before reaching the Couette flow solution. The variation of the maximum velocity (at the surface) is presented in terms of Ma in Figure 15, for both conducting and adiabatic cases. This figure confirms that the thermal boundary condition doesn't play an important role in the surface velocity, at least up to $Ma = 750$ for $Pr = 0.015$.

We must mention two asymptotic studies performed independently by Sen & Davis [1982] and by Strani *et al.* [1983], devoted to layers of large extent ($A \to \infty$). In this limiting case, the flow pattern can be divided in three parts: the core region (far from the walls) where the flow is rather simple and the two end wall regions where the flow has to turn. These two studies use asymptotic solutions (in powers of 1/A) for the velocity and the temperature in the core and in the end wall regions, and use a matching technique. Strani *et al.* [1983] results, in particular, exhibit a difference between the flow

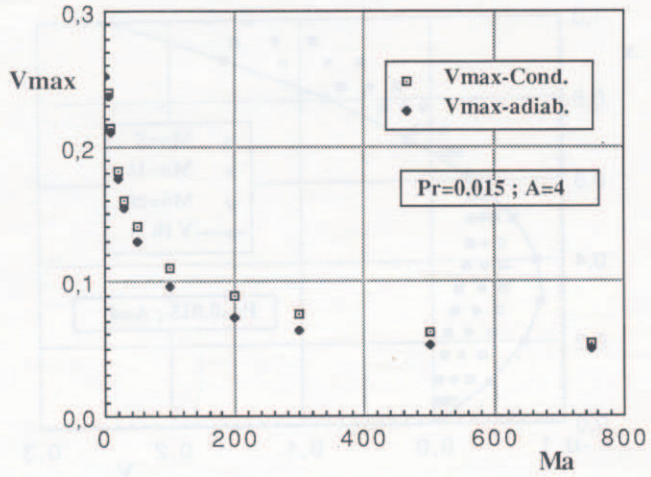

Fig. 15. — Evolution of v_{max} in terms of Ma.

structure in the two end wall regions; the velocity and the horizontal temperature gradient are higher on the cold side and the difference between the values on the cold and hot sides is proportional to Re_M and reaches 10% for $Re_M \approx 100$. This asymptotic study also shows the existence of a vortex on the cold side. Strani *et al.* [1983] also carried out numerical solutions in the case $Pr=1$ and for $A=5$, and their results for $Re_M=10$ at $y=A/2$ are in good agreement with the Couette flow solution. This agrees well with our results in Figure 12, that show the same type of agreement for $A=4$, $Ma=1$ and $Pr=0.015$, *i. e.* for $Re_M=67$.

One can say in conclusion, that our results in Figure 10 for $A=4$ and $Pr=0.015$ show, in agreement with those of Strani *et al.* [1983], that the flow field rapidly differs from the Couette flow solution as Re_M increases; in fact this behaviour is observed as soon as $Ma \geqq 5$, *i. e.* for $Re_M \geqq 333$. For such high values of Re_M, the results of the stability theories which use this basic flow (like the one of Smith & Davis [1983]), have to be applied with caution.

5.3. Coupling between the two modes of convection

It was not the goal of the present paper to make an exhaustive study of the coupling between volume- and surface-driven convections; but we were asked by one of the reviewers to speculate about the result of such a coupling. For this interesting but difficult purpose, we must at least distinguish between the two extreme cases where one of the two convections dominates (the other only behaving as a disturbance), and the most complex case where the two convections have about the same intensity and act in opposite direction. In this last case any speculation is hazardous.

Several studies, mainly experimental, have already been devoted to the coupling effect (*see* for example [Ostrach & Pradhan, 1978]; [Schwabe, 1981]; [Preisser *et al.*, 1983]; [Ochiai *et al.*, 1984]) even if these studies concern fluids with $Pr>1$. Concerning small-Prandtl-number fluids, a numerical study has been performed [Chang & Wilcox, 1976],

for a cylinder (height/diameter = 1) for Pr = 0.023 and Ma = 350 with Gr = 77.5 et Gr = 775, and recently by Bergman & Keller [1988] for A = 2, Pr = 0.01, $10^4 \leqq Ra \leqq 10^6$, with Ma = 0 and Ma = $\pm 10^4$.

We thus limit our speculation to the perturbating role of thermocapillary convection on buoyancy convection. Two cases can be considered depending on whether thermocapillary convection generates a flow which increases the motion induced by the natural convection alone (Ma > 0), or, on the contrary, limits it. In the first case, one could think that the velocity raising favours the onset of oscillatory instabilities described in Figure 4, as they have a dynamical origin. However, the preliminary computations we performed to confirm this speculation show that, contrary to this expectation, the stability is reinforced, *i. e.* the Gr_c increases with Ma (e. g. for Pr = 0.01 Gr_C is equal to 7,642, 7,829 and 8,021, when Ma is respectively −0.1, 0. and 0.1). We first tried to attribute this stabilizing effect to the positive thermal stratification induced by the thermocapillary motion on the top of the fluid layer. For negative Ma, the isotherm deformation is inverted, giving a less stable situation. For such a coupling effect between a vertical temperature gradient and a parallel flow, one can refer to the monography by Platten & Legros [1984].

This behaviour would agree with the Bergman & Keller [1988] results for higher values of Ma. Indeed, the structure of the streamlines and isotherms obtained by these authors in the case Ma = 0 can be compared to the ones for Ma = $\pm 10^4$ (*see* their Figs. 4 *a*, *b* and *c*). For Ma = 10^4, the mass flow rate increases and is associated with a strong positive (stabilizing) thermal stratification. For Ma = -10^4, the sense of the main flow is inverted (thermocapillary effects being dominant) and the thermal stratification becomes negative (destabilizing).

However, a more realistic interpretation for the increase of Gr_c with Ma, in our case, certainly lies in the displacement of the inflexion point of the basic velocity profile. This velocity is given by:

$$v(x) = v_{RF}(x) + Re_M/Gr\, v_M(x);$$

and the elevation of the inflexion point, by:

$$x_{inf} = 5/8 + 1.5\ Re_M/Gr.$$

For positive Re_M (or Ma), $x_{inf} \geqq 1$ as soon as $Re_M \geqq Gr/4$; then the basic velocity profile does not contain an inflexion point (a more stable situation). Note in addition that, negative Re (or Ma), $x_{inf} \leqq 0$ as soon as $Re_M/Gr \leqq -5/12$; thus in that case, the basic velocity profile also does not contain an inflexion point. This means that the flow also re-stabilizes for large negative Re_M, at least for $Re_M/Gr \leqq -5/12$.

All these behaviours have to be confirmed by direct simulations; that will be done in the near future.

6. Conclusion

We presented a set of results, obtained from the stability theory and by a direct numerical simulation, which show the existence of 2D oscillatory regimes occuring in

differentially heated horizontal fluid layers, with small-Prandtl-numbers, as for metallic melts. These oscillations occur for quite small temperature gradients ($Gr \approx 2 \times 10^4$), similar to the ones existing in real crystal growth experiments by the directional solidification (horizontal Bridgman) technique, or in more fundamental experiments such as the ones performed by Hurle *et al.* [1974] with liquid gallium in small boxes, with $2 \leqq A \leqq 5$. At the threshold, the frequencies of these 2D oscillations, based on ν/H^2, are of the order of 9 for $A \to \infty$ and of 13 for $A = 4$ (after Winters [1987]); they agree well with the frequencies found by Hurle *et al.* [1974].

We can thus consider that there is at least one mechanism, due to natural convection in a one-component melt, which can qualitatively explain the stable oscillations observed in real systems. This mechanism is essentially dynamical, as it also exists for $Pr = 0$ where the temperature field is completely frozen. Of course, in the real cases, where $Pr \neq 0$, this mechanism is coupled with some others (like confinement, thermocarpillary convection, etc.), which can modify the threshold for the onset of oscillations.

The interpretation of the experiments is not simple! Indeed, the stability results show that two very different oscillatory regimes are possible, one 2D and the other 3D. The 2D oscillatory regime would be dominant for small Pr: $Pr \leqq 0.004\,5$, in the adiabatic case, and $Pr \leqq 0.077$, in the conducting case. But the neutral stability curves are also affected by the confinement effect in the y-direction (for the 2D and 3D modes) and in the z-direction (for the 3D modes); the confinement would substantially modify the Pr value at which the neutral 2D and 3D stability curves intersect. We can note that the frequencies of each of these modes are very different. Thus, a correct interpretation of any experiment will require a precise knowledge of the influence of the confinement and of the thermal boundary conditions at the free-surface.

The computations performed for thermocapillary convection alone, for $A = 4$, showed that as soon as Ma is greater than a few units, the flow cannot reach a fully-developed state (Couette solution) in cavities with moderate aspect ratios which correspond, for example, to the experiments of Hurle *et al.* [1974]. One would probably need to take into account this acceleration of the basic flow if one wishes to use the stability results of Smith & Davis [1983] which exhibit oscillatory regimes in cavities of larger and larger extent as $Pr \to 0$ ($\lambda_z \approx Pr^{-1/2}$). However, we cannot exclude the possibility that the thermocapillary convection can play a certain role, even in confined cavities, by changing the velocity level in the fluid layer.

We also wish to note the fundamental interest of the hydrodynamic stability of a horizontal layer with a free-surface, as it presents the possibility for the two oscillatory (2D and 3D) modes to co-exist for a certain Pr, with quite different frequencies.

Acknowledgements

The authors wish to warmly thank J. J. Favier and his co-workers, K. H. Winters and G. Iooss, for several interesting discussions that permitted a more rapid achievement of this study. The authors also thank the team of Point d'Accès Saint-Charles, directed

Ky Dang Quoc, for precious help in using computational equipments and the C.N.E.S. (Division Microgravité Fondamentale et Appliquée) for its decisive financial support.

REFERENCES

BEN HADID H., ROUX B., 1986, Oscillatory buoyancy-driven flow in horizontal liquid-metal layer. 6th European Symposium Materials Sciences in Microgravity conditions, *ESA-SP*-256, 477-485.

BEN HADID H., ROUX B., RANDRIAMAMPIANINA A. CRESPO E., BONTOUX P., 1986, Onset of Oscillatory Convection in Horizontal Layers of Low-Prandtl-Number Melts, NATO-A.S.I. series, Plenum Press, New York.

BIRIKH R. V., 1966 *a*, *J. Appl. Math. Mech.* (P.M.M.), **30**, 356-361.

BIRIKH R. V., 1966 *b*, Thermocapillary convection in a horizontal layer of liquid, *J. Appl. Mech. Tech. Phys.*, **7**, 43-48.

BONTOUX P., 1978, Contribution à l'étude des écoulements visqueux en milieu confiné; analyse et optimisation des méthodes numériques de haute précision, *Thèse de Doctorat*, Université d'Aix-Marseille II.

BRENIER B., ROUX B., BONTOUX P., 1986, Comparaison des méthodes Tau-Chebyshev et Galerkin dans l'étude de stabilité des mouvements de convection naturelle, *J. Méc. Théor. Appl.*, **5**, 95-119.

BERGMAN T. L., KELLER J. R., 1988, Combined buoyancy, surface tension flow in liquid metals, *Num. Heat Transf.*, **13**, 49-63.

CAMEL D., TISON P., FAVIER J. J., 1986, Marangoni flow regimes in liquid metals, *Acta Astr.*, **13**, 723-726.

CARRUTHERS J. R., 1968, Thermal Convection in Horizontal Crystal Growth, *J. Crystal Growth*, **2**, 1-8.

CARRUTHERS J. R., 1977, Thermal Convection Instabilities Relevant To Crystal Growth from Liquids. In: Preparation and Properties of Solid State Materials, Vol. 3, Ed. Wilcox and Lefever. M. Dekker, New York.

CARRUTHERS J. R., WINEGARD W. C., 1967, Thermal Convection and Solute Segregation during Horizontal Melting and Solidification, *J. Phys. Chem. Solid*, Supplement No. **1**, 645-649.

CHENG C. E., WILCOX W. R., 1976, Analysis of surface tension driven flow in floating zone melting, *Int. J. Heat Mass Transfer*, **19**, 355-366.

COLE G. S., WINEGARD W. C., 1964, Thermal Convection During Horizontal Solidification of Pure Metals and Alloys, *J. Institute. Metals*, **93**, 153-164.

CROCHET M. J., GEYLING F. T., VAN SCHAFTINGEN J. J., 1983, Numerical Simulation of the horizontal Bridgman growth of a Gallium Arsenide crystal, *J. Crystal Growth*, **65**, 166-172.

FAIRWEATHER G., MITCHELL A. R., 1967, *S.I.A.M. J. Num. Anal.*, **4**, 2-15.

FAVIER J. J., ROUZAUD A., COMERA J., 1987, Influence of various hydrodynamic regimes in melts on solidification interface, *Rev. Phys. Appl.*, **22**, 195-200.

GILL A. E., 1974, A Theory of Thermal Oscillations in Liquid Metals, *J. Fluid Mech.*, **64**, 577-588.

GRESHO P. M., UPSON C. D., 1983, Application of a modified finite element method to the time-dependent thermal convection of a liquid metal, Law. Liv. Nat. Lab. Report UCRL-88990.

HART J. E., 1972, Stability of thin non-rotating Hadley circulations, *J. Atmos. Sci.*, **29**, 687-697.

HART J. E., 1983, A note on the Stability of Low Prandtl Number Hadley Circulation, *J. Fluid Mechan.*, **132**, 271-281.

HURLE D. T. J., 1967, Thermo-Hydrodynamic Oscillations in Liquid Metals: The Cause of Impurities Striations in Melt-Grown Crystals, *J. Phys. Chem. Solid*, Supplement n° 1, 659-663.

HURLE D. T. J., JAKEMAN E., JOHNSON C. P., 1974, Convective Temperature Oscillations in Molten Gallium, *J. Fluid Mech*, **64**, 565-576.

LAURE P., 1987, Étude des mouvements de convection dans une cavité rectangulaire avec un gradient de température horizontal, *J. Méc. Théor. Appliquée*, **6**, p. 351-382.

LAURE P. ROUX B., 1987, Synthèse des résultats obtenus par l'étude de stabilité des mouvements de convection dans une cavité horizontale de grande extension, *C.R. Acad. Sci*, série II, **305**, 1137-1143.

NAPOLITANO L., 1982, Surface and buoyancy driven free convection, *Acta Astron.*, **9**, 199-215.

OCHIAI J., KUWAHARA K., MORIOKA M., ENYA S., SEZAKI K. MAEKAWA T., I. TANASAWA I., 1984, Experimental study on Marangoni convection. Fifth European Symposium on Material Sciences in Space, *ESA-SP-222*, 291-295.

OSTRACH S., 1976, Convection Phenomena at reduced gravity of importance for materials processing, Second European Symposium on Material Sciences in Space, *ESA-SP-114*, 41-56.

OSTRACH S., PRADHAN A., 1978, Surface-Tension induced convection at reduced gravity, *AIAA J.*, **16**, 419-424.

PIMPUTKAR S. M., OSTRACH S., 1981, Convective Effects in Crystals Grown from Melts, *J. Crystal Growth*, **55**, 614-646.

PLATTEN J. K., LEGROS J. C., 1984, *Convection in liquids*, Springer Verlag, Heidelberg.

POLEZHAEV V. I., 1984, Hydrodynamics, Heat and Mass Transfer During Crystal Growth, In *Crystal*, Springer Verlag.

POLEZHAEV V. I., DUBOVIK K. G., NIKITIN S. A. PROSTOMOLOTOV A. I., FEDYUSKIN A. I., 1981, Convection during crystal growth on Earth and in Space, *J. Crystal Growth*, **52**, 465-470.

PREISSER F., SCHWABE D., SCHARMANN A., 1983, Steady and oscillatory thermocapillary convection in liquid columns with free cylindrical surface, *J. Fluid Mech.*, **126**, 545-567.

ROUX B., GRONDIN J. C., BONTOUX P., GILLY B., 1978, On a high-order accurate method for the numerical study of natural convection in a vertical square cavity, *Num. Heat Transfer*, **1**, 331-349.

ROUX B., BONTOUX P., LOC T. P., DAUBE O., 1979, Optimisation of Hermitian methods for N.S. equations in vorticity and streamfunction formulation. *Lect. Notes in Math.*, 771, 450-468, Springer Verlag.

SCHWABE D., 1981, Marangoni effects in crystal growth melts, *Physico Chem. Hydrod.*, **2**, 263-280.

SEN A. K., DAVIS S. H., 1982, Steady thermocapillary flows in two-dimensional slots, *J. Fluid Mech.*, **121**, 163-186.

STRANI M., PIVA R., GRAZIANI G., 1983, Thermocapillary convection in a rectangular cavity: asymptotic theory and numerical simulation. *J. Fluid Mech.*, **130**, 347-376.

SMITH M. K., DAVIS S. H., 1983, Instabilities of dynamic thermocapillary liquid layers-Part. 1. Convective instabilities, *J. Fluid Mech.*, **132**, 119-144.

UTECH H. P., BROWER W. S., EARLY S. G., 1967, Thermal Convection and Crystal Growth in Horizontal Boats, in: *Crystal Growth*, Peiser, 201-205, Pergamon Press, Oxford.

VAHL DAVIS G. de, 1986, Finite difference methods for natural and mixed convection in enclosures, in: *Heat Transfer*, **86**, 101-109, Hemisphere, Washington.

WILKE H., LÖSER W., 1983, Numerical calculation of Marangoni convection in a rectangular open boat. *Crystal Res. Tech.*, **18**, 825-833.

WINTERS K. H., 1987, Oscillatory Convection in Crystal Melts: the Horizontal Bridgman. *Proceed. 5th Int. Conf. in Thermal Problems*, Montréal, Canada, 29 June-3 July.

WINTERS K. H., 1988, Oscillatory Convection in liquid metals in a horizontal temperature gradient, submitted to *Int. J. Num. Meth. Enging.*

WINTERS K. H., CLIFE K. A., JACKSON C. P., 1987, The Prediction of Instabilities using Bifurcation Theory. Harwell Report HL86/1147. In: *Transient and Coupled System*, John Wiley, Chichester, U.K.

ZEBIB A., HOMSY G. M., MEIBURG E., 1985, High Marangoni number convection in a square cavity. *Phys. Fluids*, **28**, 3467-3476.

(Manuscript received November 24, 1987.)